THE JOURNAL OF PHYSICAL CHEMISTRY B

Article

pubs.acs.org/JPCB

Electrochemical Oxidation of Pyrogallol: Formation and Characterization of Long-Lived Oxygen Radicals and Application To Assess the Radical Scavenging Abilities of Antioxidants

Shaolin Mu*

Department of Chemistry, Yangzhou University, Yangzhou 225002, Jiangsu Province, P. R. China

Chong Chen

Laboratory Center of Yangzhou University, Yangzhou 225002, Jiangsu Province, P. R. China

ABSTRACT: Electrochemical oxidation of pyrogallol in a pH 5.0 phosphate buffer was carried out on a reduced graphene oxide/glassy carbon (RGO/GC) electrode. Reduced graphene oxide plays an important role in catalyzing the electrochemical oxidation of pyrogallol. A deep yellow film deposited on the electrode exhibits electroactivity in a wide pH range. On the basis of the experimental results from measurements of ^{1}H NMR, ^{13}C NMR, and IR spectra, there are hydroxyl, carbonyl, and aldehyde groups in the product. No visible absorption peak occurs in the UV−vis spectrum of the product, and its molecular weight is lower than that of the dipolymer but higher than that of the monomer. Therefore, the film is neither a polymer nor a dipolymer and is only a product of pyrogallol oxidation with oxygen radicals. No tendency toward the decay of the ESR signal intensity of the electrogenerated film deposited on the RGO/graphite electrode was observed after 210 days. Electrogenerated film was used as a radical source to test the radical scavenging abilities of ascorbic acid, catechin, and catechol in aqueous solutions based on the ESR signal intensity. The result indicates that ascorbic acid and catechin can scavenge the free radicals, but catechol can hardly scavenge the free radicals.

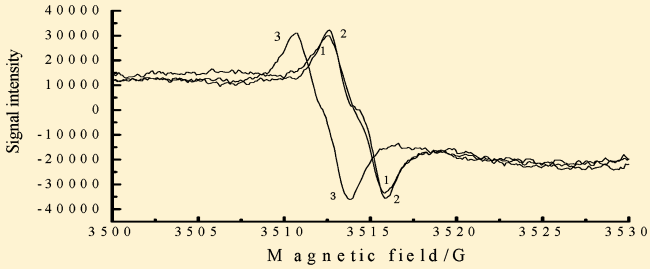

INTRODUCTION

Oxygen free radicals, including superoxide radicals and hydroxyl radicals, are very reactive species and have a very short life, for example, the half-life of a hydroxyl radical is ca. 10^{-9} s.[1] In this case, oxygen free radicals are extremely difficult to be detected directly by conventional methods. Generally, the electron spin resonance (ESR) spin trapping method is used to detect the hydroxyl radical or other oxygen radicals. Spin traps, nitroso and nitrones compounds such as 5,5-dimethyl-3,4-dihydropyrrole *N*-oxide (DMPO)[2,3] and *N*-*tert*-butylbenzylideneamine *N*-oxide (PBN),[4] are used to react with oxygen free radicals to generate a relative stable nitroxide free radical, i.e., spin adduct, which is then detected by ESR spectroscopy.[2−8]

The hydroxyl radical is the most reactive oxygen radical of all the reactive oxygen species that are normally produced in organisms being involved in various biological reactions. The hydroxyl radical can react with every cellular component, particularly lipids and nucleic acids.[9,10] Therefore, reactive oxygen species often cause oxidative stress, which is related to aging and diseases such as cancer, cardiovascular disease, Alzheimer's disease, and Parkinson's disease.[10] Recently, study on antioxidants, including polyphenols, two-hydroxy (catechol, resorcinol) and three-hydroxy (pyrogallol, phloroglucinol) phenols, has received a great deal of attention, because they can effectively scavenge free radicals.[11−16] As a result, these antioxidants play an important role in preventing or lowering the risk of various diseases caused by oxygen free radicals.

The radical scavenging abilities of antioxidants were generally assessed on the basis of their capacity to scavenge free radicals. To assess accurately such radical scavenging ability, a stable free radical species is necessary. As mentioned above, the oxygen radicals have a very short life; therefore, 2,2-diphenyl-1-picrylhydrazyl (DPPH) is generally used as a free radical source to assay the radical scavenging ability of antioxidants using UV−vis.[17−19] This method was carried out in a mixture of an antioxidant and DPPH. After the redox reaction between them, the maximum absorbance at 516 nm corresponding to the DPPH intense color was measured for the mixture using a UV−vis spectrometer. Except DPPH, 2,2′-azinobis(3-ethylbenzothiazoline-6-sulfonic acid) diammonium salt (ABTS),[20] and ferric reducing/antioxidant power (FRAP)[21] assays are also used to assess the radical scavenging abilities of antioxidants based on measurements of the visible spectra, but their experimental procedure is more complicated. Recently, we found that poly(aniline-*co*-*o*-aminophenol) has a stable and strong ESR signal in the near neutral aqueous solutions, which

Received: June 15, 2012
Revised: September 20, 2012
Published: September 25, 2012

dx.doi.org/10.1021/jp3059189 | *J. Phys. Chem. B* 2012, 116, 12567−12573

thus has been used as a probe for radical scavenging abilities based on direct ESR measurements.[22,23] The experimental results demonstrated that the antioxidants can effectively scavenge the free radicals of poly(aniline-*co*-*o*-aminophenol); however, pyrogallol with very strong antioxidant activity not only cannot scavenge the free radical but also makes the ESR signal intensity of poly(aniline-*co*-*o*-aminophenol) increase pronouncedly because of formation of a new free radical on the poly(aniline-*co*-*o*-aminophenol) in the electrolytic process of pyrogallol.[23] The latter enhanced the ESR signal intensity of poly(aniline-*co*-*o*-aminophenol). In this work, we report the formation and characterization of this new free radical in more detail. It was found that this free radical has a very long life, which can be used as a probe for radical scavengers to test the radical scavenging abilities of antioxidants, and in particular, the product of pyrogallol oxidation is not a polymer.

EXPERIMENTAL SECTION

Pyrogallol and other chemicals used were of analytical reagent grade. They were purchased from Sinopharm Chemical Reagent Co., Ltd.. Doubly distilled water was used to prepare all solutions. pH values of the solutions were determined with a PXD-12 pH meter.

A glassy carbon (GC) disk electrode (3 mm diameter) was polished with alumina slurry of 0.3 μm diameter on a polish cloth and then sonicated in a distilled water bath for 15 min before use. Graphene oxide (GO) nanosheets were prepared from natural graphite powers by a modified Hummers' method.[26] An aqueous dispersion of pristine GO sheets (0.05 wt %) was prepared by sonicating for 90 min. A 5 μL aqueous dispersion of GO sheets was dropped on a GC disk that was then allowed to dry at 40 °C to form a GO/GC electrode. The GO/GC electrode was reduced at −1.0 V for 90 min in a 0.30 M NaH_2PO_4 solution of pH 4.15 to form a reduced graphene oxide/GC electrode (i.e., RGO/GC electrode).[25,26] In addition, a graphite fiber (0.7 mm diameter) coated with GO sheets was also reduced at the same conditions as mentioned above to form a RGO/graphite electrode that was used to determine ESR spectra because the appropriate GC fiber was not available. A traditional three-electrode system consisting of a RGO/GC or RGO/graphite working electrode, a platinum foil counter electrode, and a saturated calomel reference electrode (SCE) was used for electrochemical experiments that were performed on a CHI 407 workstation.

UV−vis spectra of the samples were measured in a quartz cuvette with a path length of 1 cm using a Shimadzu 2550 double-beam spectrophotometer. ^1H and ^{13}C NMR spectra of the samples were recorded, respectively, on a 600 and 150 MHz Bruker spectrometer at 301 K in dimethylsulfoxide-d_6 (DMSO-d_6) in a 5 mm diameter NMR tube. The electrogenerated film/RGO/GC electrode was first immersed in methanol, and then this solution was dropped on a pressed KBr pellet. The IR spectrum of the dried KBr pellet containing the sample was measured using a Bruker IFS 66/s spectrometer. ESR measurements were performed using a Bruker A300 spectrometer operating in the X band (9.862 GHz) at 25 °C. The microwave power for the ESR measurements of the samples was set at 63.5 mW; the modulation frequency was set at 100.00 kHz; the modulation amplitude was set at 1.0 G; receiver gain was 1.00×10^3; time constant was 163.84 ms; sweep time was 167.77 s. Samples deposited on the RGO/graphite electrodes with approximately 3.5 cm length and 0.7 mm diameter were obtained via electrolysis of pyrogallol under a constant potential of 0.85 V, in which a total charge of 16 C was consumed. After electrolysis, this electrode was washed with distilled water, dried, sealed in a glass capillary by heating, and used to measure the ESR spectra. This electrode was kept at room temperature when not in use. Bruker Co. provides a g factor marker with $S^{3/2}$. Its g factor is 1.9800 ± 0.0006. The molecular weight of the sample was measured by mass spectrometry (ESI-MS) using a LCQ Deca XP Max mass analyzer with an ion source of electrospray ionization (ESI). The ESI-MS was in positive mode. The sample was dissolved in methanol. The solution was filtered with 0.45 μm syringe filters before injection into the column.

RESULTS AND DISCUSSION

Electrochemical Oxidation of Pyrogallol, and Electrochemical Properties of the Product. Electrochemical oxidation of pyrogallol was first carried out using cyclic voltammetry with 20 cycles between −0.20 and 0.90 V in a solution containing 50.0 mM pyrogallol and 0.20 M phosphate buffer with pH 5.0. In order to simplify, only the first 10 cycles are shown in Figure 1A and 1B. Figure 1A shows cyclic

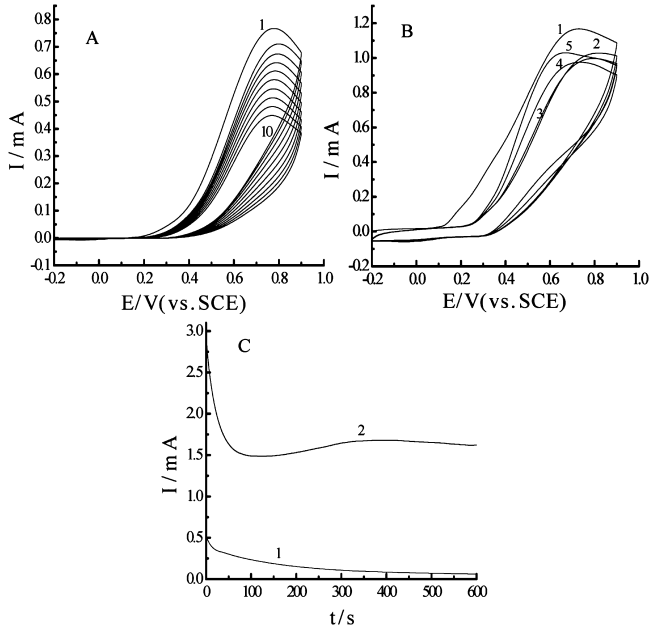

Figure 1. Cyclic voltammograms of pyrogallol in a solution consisting of 50.0 mM pyrogallol and 0.20 M phosphate buffer with pH 5.0: (A) on a GC electrode, (1) 1st cycle, (10) 10th cycle; (B) on a RGO/GC electrode, (1) 1st cycle, (2) 2nd cycle, (3) 3rd cycle, (4) 5th cycle, and (5) 10th cycle, at a scan rate of 60 mV s^{-1}. (C) Electrolysis of pyrogallol at a constant potential of 0.85 V (vs SCE) (1) on a GC electrode and (2) on a RGO/GC electrode.

voltammograms of pyrogallol on a GC electrode. There is an anodic peak at 0.78 V in Figure 1A, which is caused by pyrogallol oxidation. Clearly, its peak current decreases with an increasing number of cycles, indicating that the product with low conductivity was formed on the GC electrode. Figure 1B shows cyclic voltammograms of pyrogallol on a RGO/GC electrode in which an anodic peak appears at 0.73 V for the 1st cycle, which is more negative than that on curve 1 in Figure 1A. Moreover, after the 3rd cycle (curve 3) the anodic peak shifts gradually toward more negative potentials with increasing number of cycles. At the 10th cycle, the anodic peak shifts to

dx.doi.org/10.1021/jp3059189 | J. Phys. Chem. B 2012, 116, 12567−12573

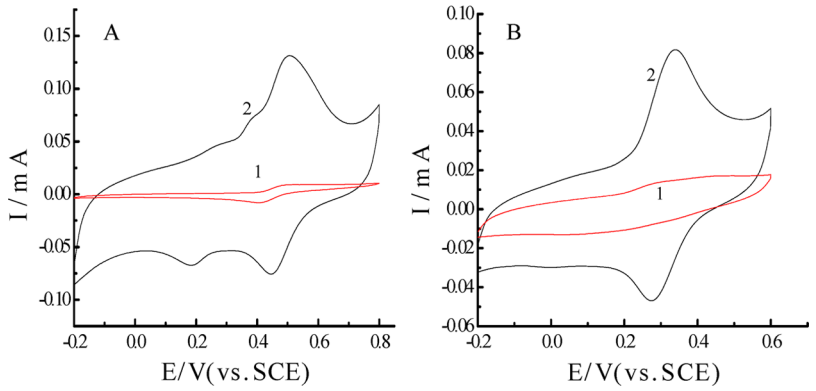

Figure 2. Cyclic voltammograms of the electrogenerated film prepared by cyclic voltammetry shown in Figure 1: (A) in a 0.20 M H_2SO_4 solution and (B) in a 0.30 M Na_2SO_4 of pH 5.0 (1) deposited on a GC electrode and (2) deposited on a RGO/GC electrode at a scan rate of 60 mV s^{-1}.

0.65 V. In comparison with Figure 1A, it is clear that the peak potential in Figure 1B shifts toward more negative potentials during the electrolytic process that was caused by RGO, which catalyzed oxidation of pyrogallol due to the presence of free radicals in RGO.[24] More evidence for electrocatalysis is that the peak current on the RGO/GC electrode increases with an increasing number of cycles after the 3rd cycle in Figure 1B. Therefore, the electrolytic behavior of pyrogallol shown in Figure 1B is quite different from that in Figure 1A. However, the peak current at the RGO/GC electrode decreases slowly with time after the 13th cycle; this would be caused by the product that covered over the entire RGO surface. As a result, RGO lost its catalytic activity to pyrogallol oxidation. During the electrolytic process, the colorless solution changed gradually to deep yellow, indicating that a product was partially dissolved in the aqueous solution. After electrolysis, it was found that the product deposited on both electrodes is deep yellow. For the time being, the product deposited on the electrode is called the electrogenerated film.

To confirm the electrocatalytic oxidation of pyrogallol by RGO, electrolysis of pyrogallol was carried out at a constant potential of 0.85 V, which is advantageous to electrochemical oxidation of pyrogallol. This is because the oxidation peak of pyrogallol on the GC electrode is at 0.78 V. Curves 1 and 2 in Figure 1C show the change in the current with time during electrolysis of pyrogallol on the GC and RGO/GC electrodes, respectively. A distinct difference between curves 1 and 2 is first that the current of the RGO/GC electrode is much higher than that of the GC electrode and second that the current of curve 1 decreases with time continuously, and whereas the current of curve 2 decreases first, then increases with time, and finally decreases again with time. The decrease in the current at both electrodes after the onset of electrolysis is due to formation of the product on the electrode and the decrease in the concentration of pyrogallol around the electrode because of the quiescent solution. However, the current of curve 2 increases after approximately 100 s, which is evidence for electrocatalytic oxidation at the constant potential electrolysis, and finally, the current decreases again after approximately 420 s. The latter would be attributed to the electrogenerated film that covered the entire RGO surface as discussed above. The results shown in Figure 1C confirmed that RGO can catalyze oxidation of pyrogallol.

Figure 2 shows cyclic voltammograms of the electrogenerated film in different solutions, which was prepared by cyclic voltammetry between −0.20 and 0.90 V with 20 cycles as mentioned previously. Curves 1 and 2 in Figure 2A are cyclic voltammograms of the electrogenerated films in 0.20 M H_2SO_4 solution, which were deposited on the GC and RGO/GC electrodes, respectively. An oxidation peak at 0.50 V and a reduction peak at 0.40 V occur on curve 1; however, three oxidation peaks at 0.25 (shoulder), 0.38 (shoulder), and 0.50 V and two reduction peaks at 0.19 and 0.44 V occur on curve 2 in Figure 2A. ΔE_p for the first and third pair of redox potentials is 60 mV, respectively, indicating one-electron reaction. No corresponding reduction peak of the second oxidation peak at 0.38 V (shoulder) is observed on curve 2, indicating that this reaction is irreversible. This anodic shoulder would arise from an unstable intermediate because its shoulder current decreases slowly with increasing number of cycles. The results shown in Figure 2A indicate that the electrochemical property of the electrogenerated film deposited on the GC electrode is different from that of the electrogenerated film deposited on the RGO/GC electrode. Curves 1 and 2 in Figure 2B are cyclic voltammograms of the electrogenerated film in 0.30 M Na_2SO_4 solution of pH 5.0. The redox peaks almost disappear on curve 1, and only one pair of redox peaks occurs on curve 2, in which an oxidation peak appears at 0.34 V and its corresponding reduction peak appears at 0.28 V. Clearly, the electrochemical behavior of the electrogenerated film in 0.20 M H_2SO_4 solution is quite different from that in a solution of pH 5.0. The ΔE_p on curve 2 in Figure 2B is also 60 mV. Moreover, the redox potentials of both electrodes in 0.20 M phosphate buffer of pH 5.0 shift toward more negative potentials compared to those of the electrogenerated film in 0.20 M H_2SO_4 solution. The above results indicate that the electrochemical property of the electrogenerated film is related to pH value, i.e., the redox of the electrogenerated film needs participation of protons. A pronounced feature in Figure 2 is that the area of the cyclic voltammogram of curve 2 is much larger than that of curve 1 in both solutions, which is caused by the amount of electrogenerated film deposited on the RGO/GC electrode being greater than that of the electrogenerated film deposited on the GC electrode at the same experimental conditions. This result is similar to electrochemical polymerization of *o*-aminophenol[26] and *o*-phenylenediamine[27] on the bare GC and RGO/GC electrodes. Therefore, electrolysis of pyrogallol at a constant potential confirmed that reduced graphene oxide can catalyze the electrochemical oxidation of pyrogallol.

All electrogenerated films used in the following experiments were prepared by electrolysis of pyrogallol under a constant

dx.doi.org/10.1021/jp3059189 | J. Phys. Chem. B 2012, 116, 12567−12573

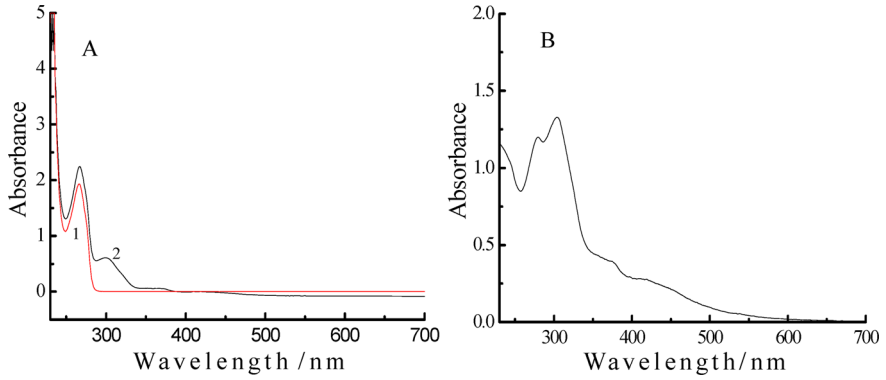

Figure 3. UV−vis spectra of (A) pH 5.0 phosphate buffer containing 1 mM pyrogallol (1) and after electrolysis (2) and (B) the electrogenerated film dissolved in methanol.

potential of 0.85 V in the solution containing 50.0 mM pyrogallol and 0.20 M phosphate buffer with pH 5.0.

UV−Vis Spectra and Molecular Weight Measurement. Curves 1 and 2 in Figure 3A show UV−vis spectra of pyrogallol in a pH 5.0 phosphate buffer before and after electrolysis, respectively. A peak at 266 and 267 nm occurs on curves 1 and 2, respectively. However, a new peak at 299 nm occurs on curve 2, which derives from the soluble product of pyrogallol oxidation after electrolysis. It was found that the solution after electrolysis changed from colorless to deep yellow. The soluble product does not correspond to the electrogenerated film, which is yellow as no absorption could be observed in the visible range on curve 2 of Figure 3A. Figure 3B is the UV−vis spectrum of the electrogenerated film dissolved in methanol; the color of the solution is deep yellow. The two peaks at 279 and 304 nm in Figure 3B correspond to the first peak (267 nm) and second peak (299 nm) on curve 2 in Figure 3A, respectively, i.e., peak position shifts toward higher wavelengths, which was caused by the different solvents. In addition, a weak broad wave around 410 nm occurs in Figure 3B. This means that the molecular structure of the product dissolved in electrolytic solution during electrolytic process is slightly different from the electrogenerated film deposited on the RGO/GC electrode.

Figure 4 shows the result of molecular weight measurement. The main peak occurs at 212, which is the molecular weight of the electrogenerated film deposited on the RGO/GC electrode, which is a positive ion with the free radical. This is because the product was obtained by electrochemical oxidation that led to formation of the positive ions. Generally, fragments are seldom produced in ESI because ESI is an extremely gentle ionization method; consequently, weak bonds are often preserved. As can be seen ftom Figure 4, the peaks with m/z lower and higher than 212 possess rather low relative abundance compared to the main peak, which hence would be attributed to side products formed in the electrolytic process of pyrogallol. This molecular weight is lower than that of pyrogallol dipolymer, indicating that its conjugated chain is low.

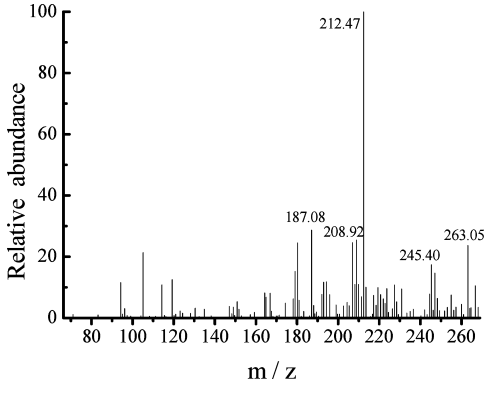

Figure 4. Mass spectrum (ESI-MS positive mode) of the electrogenerated film dissolved in methanol.

FTIR Spectrum. Figure 5 shows the FTIR spectrum of the electrogenerated film in which two peaks at 3648 and 3315 cm^{-1} are assigned to the O−H stretching vibrations. The two peaks at 2927 and 2854 cm^{-1} in Figure 5 are attributed to the CH stretching vibrations of the −CHO group in aldehydes, i.e., Fermi resonance, because two bands in aldehydes are often observed near 2900 and 2700 cm^{-1}.[28a] The peak at 1735 cm^{-1} is assigned to the carbonyl group in the electrogenerated film because the C═O stretching vibrations in aldehydes are in the range 1725−1695 cm^{-1}.[28a] The peaks at 1527 and 1462 cm^{-1} are indicative of C═C stretching vibrations of the benzene ring because the aromatic C═C stretching vibrations are in the range 1625−1430 cm^{-1}.[28a] A peak at 1383 cm^{-1} is assigned to the C−O−H deformation because the C−O−H deformation in phenols is in the range 1390−1310 cm^{-1}.[28a] A peak at 1256 cm^{-1} may be attributed to C−OH stretching vibrations in phenols.[28a] A peak at 1020 cm^{-1} is assigned to in-plane C−O bending vibrations. A peak at 843 cm^{-1} is attributed to the CH out-of-plane deformation in tetrasubstituted benzenes.[28a] A peak at 657 cm^{-1} would be assigned to C−C−CHO bending vibrations in aldehydes due to its bending is in the range 695−

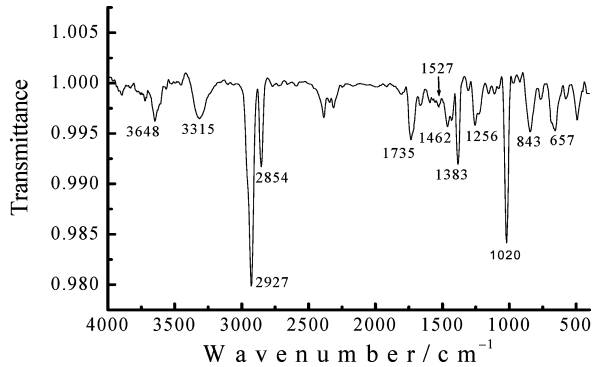

Figure 5. FTIR spectrum of the electrogenerated product dissolved in methanol that was dropped on a pressed KBr pellet.

dx.doi.org/10.1021/jp3059189 | J. Phys. Chem. B 2012, 116, 12567−12573

635 cm^{-1}.[28a] The IR spectrum shown in Figure 5 indicates that hydroxyl, carbonyl, and aldehyde groups are present in the electrogenerated film.

NMR Spectra. ^1H NMR data of the electrogenerated film are presented as follows: ^1H NMR (600 MHz, DMSO) δ 15.26 (s, 1H), 10.54 (s, 1H), 9.37 (s, 1H), 9.34 (s, 1H), 7.33 (d, J = 11.3 Hz, 1H), 7.06 (d, J = 9.4 Hz, 1H), 6.89 (s, 1H), 6.73 (dd, J = 11.3, 9.4 Hz, 1H).

The main peaks are discussed here. A strong peak at 6.89 ppm is attributed to the hydroxyl proton resonance, which corresponds to one proton based on its area under the peak. The peaks at 6.73, 7.06, and 7.33 ppm would be ascribed to the aromatic proton resonance. However, the situation is more complicated because the side products are probably formed in the electrolysis of pyrogallol. A peak of the OH proton resonance of phenol in DMSO occurs at 9.3 ppm.[29] Therefore, the peaks at 9.37 (its integration is 0.76) and 9.34 (its integration is 1.00) ppm are attributed to the OH proton resonance of the aromatic ring in the electrogenerated film. A peak at 10.54 ppm is assigned to the CHO proton resonance because the CHO proton resonance of aldehydes generally occurs at about approximately10 ppm.[28b] The ^1H NMR spectrum of the enol form of acetylacetone exhibits a peak at 15.3 ppm.[30] Therefore, a strong peak at 15.26 ppm is attributed to the fact that the hydrogen atom is characteristic of the hydrogen bonded to the oxygen of the carbonyl group, which will be discussed later. This peak corresponds to one proton based on its area under the peak.

To confirm the presence of the carbonyl group, ^{13}C NMR of the electrogenerated film was done. Its spectrum shows that a peak at 182.1 ppm occurs in the ^{13}C NMR spectrum, which is characteristic of the C═O group. Therefore, spectra of ^1H NMR and ^{13}C NMR demonstrated that the C═O group is included in the electrogenerated film.

The results from the spectra of FTIR, ^1H NMR, ^{13}C NMR, and ESR (in the next section) demonstrate the presence of hydroxyl, carbonyl, and aldehyde groups and free radicals in the electrogenerated film, and the molecular weight of the product is lower than that of its dipolymer. These results give us a hint that formation of the long-lived oxygen radicals is suggested that the dipolymer is formed first and then one benzene ring is cleaved to form 3-(3,4,5-trihydroxybenzenyl)-2,3-dihydroxypropenal during the electrochemical oxidation process. As discussed previously, several compounds would be present simultaneously in the tested sample; therefore, the main product with a molecular weight of 212 is suggested as follows

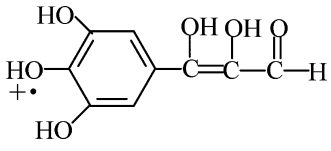

As mentioned above, the strong peak at 15.2 ppm is attributed to the hydrogen bonded to the oxygen of carbonyl group. In the above molecular structure, possible hydrogen bonds are numerous: the configuration of the double bond could be involved.

Assessment of the Radical Scavenging Abilities of Antioxidants. The electrogenerated film deposited on the RGO/graphite electrode was used as a radical source for assessing the radical scavenging abilities of the antioxidants. Therefore, the potential of the electrogenerated film in the solution containing an antioxidant is also a probe for assessing the radical scavenging ability of an antioxidant, as it is closely related to the reducing power of an antioxidant. The open-circuit potential of the electrogenerated film deposited on a RGO/graphite electrode was measured in an ESR cell[31] with a testing solution and a reference electrode of Ag/AgCl with a saturated KCl solution. Before that, the RGO/graphite electrode and reference electrode were immersed into a 0.20 M phosphate buffer solution of pH 5.0 without antioxidants, and then the change in the potential of the RGO/graphite electrode with time was measured until reaching a stable value, i.e., the equilibrium potential that is denoted as PBS at zero on the time axis in Figure 6. Curve 1 in Figure 6 shows the change

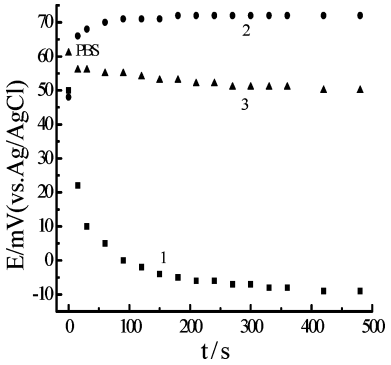

Figure 6. Change in the open-circuit potential of the electrogenerated film in 0.20 M phosphate buffer solution containing different antioxidants: (1) 10.0 mM ascorbic acid, (2) 10.0 mM catechol, and (3) 1.0 mM catechin, pH 5.0, 20 °C.

in the potential of the electrogenerated film with time in a solution containing 10.0 mM ascorbic acid and 0.20 M phosphate with pH 5.0. It is clear that the potential decreases rapidly from the equilibrium potential of 50 to 10 mV reached 30 s after moving the electrode from 0.20 M phosphate buffer solution into the solution containing ascorbic acid and then decreases slowly with time to −9 mV at 480 s. The result shown in curve 1 demonstrates that the electrogenerated film was reduced by ascorbic acid. Curve 2 shows the change in the potential of the electrode in a solution containing 10 mM catechol and 0.20 M phosphate with pH 5.0. Its potential increases from the equilibrium potential of 46 to 72 mV reached 480 s after moving the electrode from 0.20 M phosphate buffer solution into the solution containing catechol, indicating that the electrogenerated film cannot be reduced by catechol. Curve 3 in Figure 6 shows the change in the potential of the electrogenerated film with time in a solution containing 1.0 mM catechin and 0.20 M phosphate with pH 5.0. Clearly, the potential decreases from the equilibrium potential of 61 to 50 mV reached 480 s after moving the electrode from 0.20 M phosphate buffer solution into the solution containing catechin, indicating that the electrogenerated film was reduced by catechin. The results shown in Figure 6 demonstrate that the three antioxidants used here have a different reducing power on the electrogenerated film.

Figure 7A shows the change in the ESR signal intensity of the electrogenerated film deposited on a RGO/graphite electrode with time. ESR spectra of curves 1, 2, and 3 show the 1st record (1st day), the 6th record after 29 days, and the 9th record after 210 days, respectively. No tendency toward the decay of the ESR signal intensity was observed after 210 days. By contrast, the ESR signal intensity of curves 2 and 3 is slightly higher than

dx.doi.org/10.1021/jp3059189 | J. Phys. Chem. B 2012, 116, 12567−12573

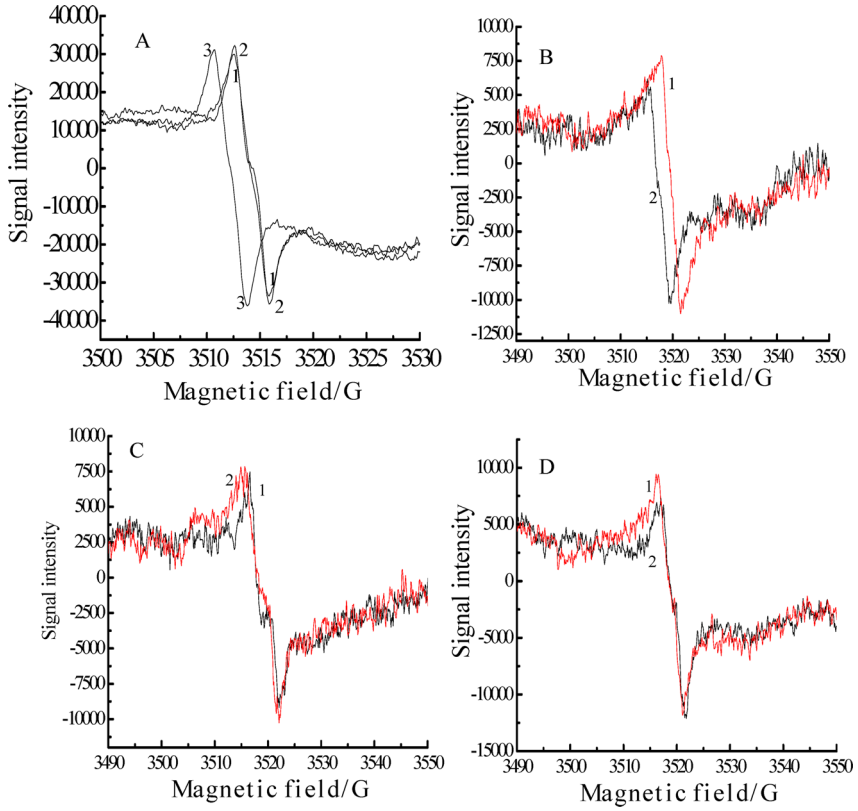

Figure 7. ESR spectra of the electrogenerated film deposited on the RGO/graphite electrodes. (A) ESR signal intensity as a function of time, (1) first record, (2) recorded after 29 days, and (3) recorded after 210 days. Radical scavenging ability: (B) (1) in 0.20 M phosphate buffer and (2) in a solution containing 0.20 M phosphate buffer and 10 mM ascorbic acid; (C) (1) in 0.20 M phosphate buffer and (2) in a solution containing 0.20 M phosphate buffer and 10 mM catechol; (D) (1) in 0.20 M phosphate buffer and (2) in a solution containing 0.20 M phosphate buffer and 1.0 mM catechin, pH 5.0.

that of curve 1. This means that the free radical in the sample has a long lifetime. To our knowledge, if the free radical in the electrogenerated film reported here is oxygen centered, according to our hypothesis, then it is the most stable one among the oxygen free radicals reported previously. The *g* value of the electrogenerated film is 2.0034, which is very close to the value of 2.0023 for a free electron and is also characteristic of organic free radicals.

Owing to the stable ESR signal, the electrogenerated film deposited on a RGO/graphite electrode can be used as a source of free radicals to assess the radical scavenging ability of an antioxidant. Curve 1 in Figure 7B–D shows the ESR spectrum of the electrogenerated film in 0.20 M phosphate buffer of pH 5.0, and then this electrode was inserted into a solution containing 10.0 mM ascorbic acid and 0.20 M phosphate buffer with pH 5.0 to measure the ESR spectrum at 6 min, which is shown in curve 2 of Figure 7B. The results in Figure 7B indicate that the ESR signal intensity of curve 2 is lower than that of curve 1. This means that ascorbic acid has a free radical scavenging ability because the electrogenerated film can be reduced by ascorbic acid, which was shown in curve 1 of Figure 6. Curve 2 in Figure 7C is the ESR spectrum of this electrode in a solution containing 10.0 mM catechol and 0.20 M phosphate buffer with pH 5.0, which was also recorded at 6 min after moving the electrode into the solution containing catechol. Figure 7C shows that the ESR signal intensity of curve 2 is slightly higher than that of curve 1 in the solution without catechol, indicating that catechol hardly scavenges the free radicals. Curve 2 in Figure 7D shows the ESR spectrum of this electrode in a solution containing 1.0 mM catechin and 0.20 M phosphate buffer with pH 5.0, which was also recorded 6 min after moving the electrode into the solution containing catechin. As can be seen in Figure 7D, the ESR signal intensity of curve 2 is lower than that of curve 1, indicating that catechin can scavenge free radicals because catechin can reduce the electrogenerated film as mentioned previously. Therefore, the results in Figure 7B–D are in good agreement with those of poly(aniline-*co*-*o*-aminophenol), which was used as a source of free radicals to assess the radical scavenging abilities of ascorbic acid, catechol, and catechin.[22,23] The results from measurements of ESR signal intensity demonstrated that ascorbic acid and catechin can scavenge the free radicals of the electrogenerated film, but catechol cannot scavenge the free radicals because they have different reducing power as shown in Figure 6. The results from the DPPH method and cyclic voltammetry show that both the scavenging ability and the reducing power of catechin are greater than those of catechol,[17] and the reducing power of ascorbic acid is greater than that of catechin.[32] According to result from the ESR spin trapping method, ascorbic acid exhibited strong hydroxyl radical scavenging activity.[33] Therefore, the results shown in Figures 6 and 7 are consistent with those reported previously. Recently, the report on analysis of the antioxidant capacities of flavonoids using different methods including DPPH and Trolox equivalent antioxidant capacity (TEAC) demonstrated inconsistent antioxidant activities depending on the assay used.[34] However, direct ESR measurement can avoid the complexity arising from the redox reactions between antioxidants and the free radical

dx.doi.org/10.1021/jp3059189 | *J. Phys. Chem. B* 2012, 116, 12567–12573

species; therefore, the ESR technique is a good tool to assess the free radical scavenging capacities of antioxidants. The above results demonstrate that the electrogenerated film can be used as a probe for radical scavenging abilities.

CONCLUSION

Electrochemical oxidation of pyrogallol in a pH 5.0 phosphate buffer was carried out on the GC and RGO/GC electrodes. RGO can catalyze the electrochemical oxidation of pyrogallol. A deep yellow film was deposited on the electrodes by electrolysis of pyrogallol, which exhibits electroactivity in a wide pH range from pH < 1 to 5.0. On the basis of the experimental results from the FTIR, UV−vis, ^{1}H NMR, ^{13}C NMR, ESR, and mass spectra, there are hydroxyl, carbonyl, and aldehyde groups and free radicals in the product, and its molecular weight is lower than that of the dipolymer of pyrogallol. Therefore, the film is neither a polymer nor a dipolymer, indicating that electrochemical oxidation of pyrogallol did not cause polymerization of pyrogallol and only caused pyrogallol to form an oxide film, that is, 3-(3,4,5-trihydroxybenzenyl)-2,3-dihydroxypropenal. ESR measurements demonstrate that the product is a stable free radical and has a long lifetime; however, the ESR signal of the electrogenerated film dissolved in THF and aqueous solution was not detected directly in our experiments. The latter may be due to the fact that the electrogenerated film dissolved in the solutions is very reactive like the conventional oxygen free radicals in the solutions reported previously. The electrogenerated film can be used for testing the radical scavenging abilities of ascorbic acid, catechin, and catechol in aqueous solutions based on measurement of the ESR signal intensity; its advantage is that the experiment is simple, fast, and accurate because the compound deposited on the electrode can be used directly as it is a stable free radical. The result indicates that ascorbic acid and catechin can scavenge free radicals, but catechol can hardly scavenge free radicals, which is similar to the results obtained using poly(aniline-*co*-*o*-aminophenol) as the free radical sources. Even though the free radical in the electrogenerated film has a long lifetime, its ESR signal is not strong enough in aqueous solutions. We are facing a significant task, i.e., how to increase the ESR signal intensity of the electrogenerated film in aqueous solutions.

AUTHOR INFORMATION

Corresponding Author

*Phone: +86 514 87975590 (ext 9413). Fax: + 86 514 87975244. E-mail: slmu@yzu.edu.cn.

Notes

The authors declare no competing financial interest.

ACKNOWLEDGMENTS

This work was supported by the Beijing National Laboratory for Molecular Science (BNLMS), 2012.

REFERENCES

(1) Pryor, W. A. *Annu. Rev. Physiol.* **1986**, *48*, 657−667.
(2) Janzen, E. G.; Kotake, Y.; Hinton, R. D. *Free Radical Biol. Med.* **1992**, *12*, 169−173.
(3) Park, P. J.; Je, J. Y.; Kim, S. K. *J. Agric. Food. Chem.* **2003**, *51*, 4624−4627.
(4) Cheng, S. A.; Fung, W. K.; Chan, K. Y.; Shen, P. K. *Chemosphere* **2003**, *52*, 1797−1805.
(5) Yamazaki, I.; Piette, L. H. *J. Biol. Chem.* **1990**, *265*, 13589−13594.
(6) Ueda, J. I.; Saito, N.; Shimazu, Y.; Ozawa, T. *Arch. Biochem. Biophys.* **1996**, *333*, 377−384.
(7) Lindsey, M. E.; Tarr, M. A. *Chemosphere* **2000**, *41*, 409−417.
(8) Berliner, L. J. *Appl. Magn. Reson.* **2009**, *36*, 157−170.
(9) Martínez-Caynela, M. *Biochimie* **1995**, *77*, 147−161.
(10) Cheng, F. C.; Jen, J. F.; Tsai, T. H. *J. Chromatogr. B* **2002**, *781*, 481−496.
(11) Mochizuki, M.; Yamazaki, S. I.; Kano, K.; Ikeda, T. *Biochim. Biophys. Acta* **2002**, *1569*, 35−44.
(12) Cren-Olive, C.; Hapiot, P.; Pinson, J.; Rolando, C. *J. Am. Chem. Soc.* **2002**, *124*, 14027−14038.
(13) Yoshioka, H.; Ohashi, Y.; Fukuda, H.; Senba, Y.; Yoshioka, H. *J. Phys. Chem. A* **2003**, *107*, 1127−1132.
(14) Thavasi, V.; Leong, L. P.; Bettens, R. P. A. *J. Phys. Chem. A* **2006**, *110*, 4918−4923.
(15) Thavasi, V.; Bettens, R. P. A.; Leong, L. P. *J. Phys. Chem. A* **2009**, *113*, 3068−3077.
(16) Quideau, S.; Deffieux, D.; Douat-Casassus, C.; Pouységu, L. *Angew. Chem., Int. Ed.* **2011**, *50*, 586−621.
(17) Hotta, H.; Nagano, S.; Ueda, M.; Tsujino, Y.; Koyama, J.; Osakai, T. *Biochim. Biophys. Acta* **2002**, *1572*, 123−132.
(18) Muzolf, M.; Szymusiak, H.; Gliszczynska-SwigŁo, A.; Rietjens, I . M. C. M.; Tyrakowska, B. *J. Agric. Food Chem.* **2008**, *56*, 816−823.
(19) Nanjo, F.; Goto, K.; Seto, R.; Suzuki, M.; Sakai, M.; Hara, Y. *Free Radical Biol. Med.* **1996**, *21*, 895−902.
(20) Muzolf, M.; Szymusiak, H.; Gliszczynska-SwigŁo, A.; Rietjens, I.; Tyrakowska, B. *J. Agric. Food Chem.* **2008**, *56*, 816−823.
(21) Faria, A.; Calhau, C.; Frettas, V.; Mateus, N. *J. Agric. Food Chem.* **2006**, *54*, 2392−2397.
(22) Yang, Y. F.; Mu, S. L. *J. Phys. Chem. C* **2011**, *115*, 18721−18728.
(23) Mu, S. L.; Chen, C. *J. Phys. Chem. C* **2012**, *116*, 3065−3070.
(24) Hummers, W.; Offernan, R. *J. Am. Chem. Soc.* **1958**, *80*, 1339−1340.
(25) Zhou, M.; Zhai, Y. M.; Dong, S. J. *Anal. Chem.* **2009**, *81*, 5603−5613.
(26) Chen, W. L.; Mu, S. L. *Electrochim. Acta* **2011**, *56*, 2284−2289.
(27) Mu, S. L. *Electrochim. Acta* **2011**, *56*, 3764−3772.
(28) (a) Lambert, J. B.; Shurvell, H .F.; Lightner, D. A.; Cooks, R. G. *Organic Structural Spectroscopy*; Prentice-Hall: Upper Saddle River, NJ, 1998; pp 180−223. (b) Lambert, J. B.; Shurvell, H .F.; Lightner, D. A.; Cooks, R. G. *Organic Structural Spectroscopy*; Prentice-Hall: Upper Saddle River, NJ, 1998; p 45.
(29) Pretsch, E.; Bühlmann, P.; Affolter, C. *Structure Determination of Organic Compounds. Tables of Spectral Data*; Springer-Verlag: Berlin, 2000.
(30) Gilbert, B. C. *Investigation of Molecular Structure, Spectroscopic and Diffraction Methods*; Bell & Hyman Ltd.: London, 1984; p 113.
(31) Zhang, F. M.; Mu, S. L. *J. Phys. Chem. B* **2010**, *114*, 16687−16693.
(32) Kilmartin, P. A.; Zou, H. L.; Waterhouse, A. L. *J. Agric. Food Chem.* **2001**, *49*, 1957−1965.
(33) Yamaguchi, F.; Yoshimura, Y.; Nakazawa, H.; Ariga, T. *J. Agric. Food Chem.* **1999**, *47*, 2544−2548.
(34) Zhang, D.; Chu, L.; Liu, Y. X.; Wang, A. L.; Ji, B. P.; Wu, W.; Zhou, F.; Wei, Y.; Cheng, Q.; Cai, S. B.; Xie, L. Y.; Jia, G. *J. Agric. Food Chem.* **2011**, *59*, 10277−10285.